Photoproduction of π^0 Mesons in Hydrogen*

L. J. KOESTER, JR., AND F. E. MILLS†
University of Illinois, Urbana, Illinois
(Received November 26, 1956)

This paper reports measurements of the total cross section from 150 to 240 Mev of incident photon energy and measurements of the 135° differential cross section from 180 to 215 Mev. A Monte Carlo evaluation of the γ-ray telescope efficiency by means of an electronic digital computer is outlined. The combined results indicate that a small but finite amount of S-state production occurs and that the angular distribution becomes flatter as the energy decreases. The latter effect is associated with production in unenhanced P-states and with a lack of electric quadrupole production. Good agreement with the Chew-Low theory is demonstrated by a comparison between the photoproduction and scattering of π^0-mesons, where the scattering cross sections are derived from those for charged mesons by charge independence.

I. INTRODUCTION

A. Theories

THE most striking result of the early photomeson experiments was that the cross section for photoproduction of neutral mesons near 300 Mev was comparable with that for charged mesons. This feature, which was discovered in the first experiment on π^0 photoproduction,[1] could not be explained by ordinary weak-coupling meson theory. Because the neutral meson possessed neither charge nor magnetic moment, the interaction would depend, in that theory, on the nucleon recoil alone. The ratio of neutral to charged meson photoproduction would then be of order $(\mu/M)^2 \approx 0.02$, where μ and M are the masses of the pion and of the nucleon, respectively.

Kaplon[2] attempted to surmount this difficulty without abandoning weak-coupling methods by introducing a Pauli-type term representing the interaction of the photon with the anomalous magnetic moment of the proton and by using the static value of this moment at all energies. He was successful in raising the π^0 photoproduction cross sections, but the associated angular distribution differed sharply from experimental results. As Bethe and de Hoffmann[3] have pointed out, Kaplon's innovation was of the nature of a strong-coupling hypothesis.

About the same time, Brueckner and Case[4] and Fujimoto and Miyazawa[5] applied strong-coupling theory characterized by nucleon isobars. The first pair of authors showed, by a classical treatment, that this theory could predict a resonant meson-nucleon interaction in an isobaric state which would yield a large cross section for π^0 photoproduction near 300 Mev. They emphasized, however, that this treatment was crude and qualitative. In the following period, a number of authors[6] achieved considerable success in describing photoproduction by means of phenomenological treatments more or less independent of specific models. Important to these methods were the consequences of charge independence outlined by Watson.[7] This principle, together with the unitarity and the invariance of the scattering matrix under time reversal led to general relations between the scattering phase shifts and photoproduction amplitudes.

In regard to π^0 photoproduction, charge independence implies that the final state $p+\pi^0$ may be represented more appropriately by a linear combination of the two possible states of total isotopic spin as follows:

$$\chi_{\frac{1}{2}}{}^{\frac{1}{2}}\phi_1{}^0 = (\tfrac{2}{3})^{\frac{1}{2}}\Psi_{\frac{3}{2}}{}^{\frac{1}{2}} - (\tfrac{1}{3})^{\frac{1}{2}}\Psi_{\frac{1}{2}}{}^{\frac{1}{2}}. \quad (1)$$

Here the product function on the left represents the individual isotopic spin projections of the proton $\chi_{\frac{1}{2}}{}^{\frac{1}{2}}$, and of the neutral pion, $\phi_1{}^0$. On the right, $\Psi_{\frac{3}{2}}{}^{\frac{1}{2}}$ and $\Psi_{\frac{1}{2}}{}^{\frac{1}{2}}$ are the projections of the states of $\frac{3}{2}$ units and of $\frac{1}{2}$ unit of total isotopic spin, respectively. The coefficients are determined by the usual rules for combining angular momenta.

Now, the scattering experiments[8] show the meson-nucleon interaction in the energy range up to a few hundred Mev to be much stronger in the isotopic spin state $\Psi_{\frac{3}{2}}$ than in the state $\Psi_{\frac{1}{2}}$. For example, the cross section for π^+ scattering by protons, which involves only $\Psi_{\frac{3}{2}}$, is about three times as large as the cross section for both ordinary and exchange scattering of π^- mesons by protons, which involves a linear combination of $\Psi_{\frac{3}{2}}$ and $\Psi_{\frac{1}{2}}$. The factor three arises when the interaction in the state $\Psi_{\frac{1}{2}}$ is negligibly small. Most of the π^0 photoproduction, therefore, can be explained in terms of the $\Psi_{\frac{3}{2}}$ scattering phase shifts, since the direct production is small.

* This research was assisted by the joint program of the Office of Naval Research and the U. S. Atomic Energy Commission.
† U. S. Atomic Energy Commission Predoctoral Fellow. Now at MURA, Madison, Wisconsin.
[1] Panofsky, Steinberger, and Steller, Phys. Rev. **86**, 180 (1952).
[2] M. F. Kaplon, Phys. Rev. **83**, 712 (1951).
[3] H. A. Bethe and F. de Hoffmann, *Mesons and Fields* (Row, Peterson, and Company, Evanston, Illinois, 1955), Vol. II.
[4] K. A. Brueckner and K. M. Case, Phys. Rev. **83**, 1141 (1951).
[5] Y. Fujimoto and H. Miyazawa, Progr. Theoret. Phys. (Japan) **5**, 1052 (1950).
[6] B. T. Feld, Phys. Rev. **89**, 330 (1953); K. A. Brueckner and K. M. Watson, Phys. Rev. **86**, 923 (1952); M. Ross, Phys. Rev. **94**, 454 (1954); S. Minami, Progr. Theoret. Phys. (Japan) **11**, 213 (1954); Hayakawa, Kawaguchi, and Minami, Progr. Theoret. Phys. (Japan) **12**, 355 (1954); Progr. Theoret. Phys. (Japan) **11**, 332 (1954).
[7] K. M. Watson, Phys. Rev. **85**, 852 (1952).
[8] For a bibliography, see Ashkin, Blaser, Feiner, and Stern, Phys. Rev. **101**, 1149 (1956).

Instead of adopting a phenomenological approach, Chew[9] developed a way of renormalizing the Yukawa theory, which is a pseudoscalar theory with pseudovector coupling. Such a theory with a moving, point source is unrenormalizable, but Chew assumed a spread-out source with infinite mass. The linear coupling in the Hamiltonian led naturally to interaction in P-states only,[10] and the P-phase shifts were predicted accurately by means of two parameters, resonance energy and source radius.

The early form of Chew's theory[11] involves interactions between the nucleon and only one meson at a time. More recently, application of the Low equations[12] has enabled Chew and Low[13] to remove the limitation to only one pion, but they retain the fixed source ("static model of the nucleon").

B. Experiments

The main results of all these more recent theoretical treatments for π^0 photoproduction, namely the P-wave part, were confirmed experimentally. The experiments published to date can be summarized briefly for reference as follows.

Silverman and Stearns[14] measured the laboratory differential cross section at 95° between incident photon energies of 215 and 310 Mev. They fitted the curve with the expression

$$d\sigma/d\Omega(95°) = \text{constant} \times (h\nu - 145)^{1.9\pm0.4},$$

where $h\nu$ is the incident photon energy in Mev. This energy dependence was consistent with production in P-states.

Cocconi and Silverman[15] measured the angular distribution of single γ rays corresponding to π^0 mesons produced by 310-Mev bremsstrahlung. Their results were consistent with a π^0 angular distribution of the form $2+3\sin^2\theta$ (pure $M1$, $P_{\frac{3}{2}}$ production) and were in contradiction with Kaplon's[2] angular distribution.

Goldschmidt-Clermont, Osborne, and Scott[16] measured total cross sections between 175 and 325 Mev and angular distributions for energy bands centered at 220, 260, and 305 Mev. They determined the three angular distribution coefficients (A, B, and C in $A+B\cos\theta+C\cos^2\theta$) at five different energies between 220 and 320 Mev. The B coefficient, corresponding to interference between S- and P-waves, was small and negative below 300 Mev. The energy dependence was consistent with production mainly in P-states.

Walker, Oakley, and Tollestrup[17] measured angular distributions at 300, 400, and 450 Mev. Subsequently, Oakley and Walker[18] measured angular distributions between 260 and 450 Mev. These angular distributions were more strongly peaked around 90° than were the earlier ones. Both of these experiments showed that the cross section went through a maximum, within the limits of experimental precision, at the same center-of-mass value of pion momentum as did the (π^+,p) scattering cross section. The excitation functions were fitted by the Watson[19] analysis with the scattering phase shifts, and by the theory of Chew and Low.[13]

Very recent measurements at forward π^0 angles by Corson, Peterson, and McDonald[20] supplement the angular distributions of Oakley and Walker. The new values are considerably higher than those obtained by fitting the Oakley and Walker data with three coefficients. The combined results of these two experiments tend to spread out the angular distribution consistent with almost pure magnetic dipole production and to make the interference term change sign well below the resonance energy.

C. S-State Production

According to what has been said thus far, the photoproduction of neutral pions in P-states is rather well understood and predicted theoretically. The S-state production, however, is a more open question. Watson[21] has derived a lower limit for this process on the basis of internal charge exchange scattering of S-state π^+ photomesons. This lower limit is really very small, and its momentum dependence is the same as that for the P-wave. One may expect, in addition, a direct production of S-state π^0 mesons from nucleon recoil. This production should vary with the first power of pion momentum instead of the third; hence it should be most easily observable very near threshold.

Neutral pion experiments near threshold are rather difficult for various reasons. The cross section is vanishingly small, and the recoil protons have too little energy to escape a target of reasonable thickness. The π^0-decay photons, however, escape easily and may be counted, the only problem being to determine which energy from the incident bremsstrahlung is responsible for an event. The method of Panofsky[1] is not suited to low-energy measurements, largely because the double gamma-ray counting rate is so small. With the precise energy control of the betatron, however, the bremsstrahlung spectrum can be unfolded by application of the "photon difference" method. This method as

[9] G. F. Chew, Phys. Rev. **94**, 1748 (1954).
[10] An explicit demonstration of this fact is given by G. C. Wick, Revs. Modern Phys. **27**, 339 (1955), see page 342.
[11] G. F. Chew, Phys. Rev. **95**, 1669 (1954).
[12] F. E. Low, Phys. Rev. **97**, 1392 (1955).
[13] G. F. Chew and F. E. Low, Phys. Rev. **101**, 1570, 1579 (1956).
[14] A. Silverman and M. Stearns, Phys. Rev. **88**, 1225 (1952).
[15] G. Cocconi and A. Silverman, Phys. Rev. **88**, 1230 (1952).
[16] Goldschmidt-Clermont, Osborne, and Scott, Phys. Rev. **97**, 188 (1955).
[17] Walker, Oakley, and Tollestrup, Phys. Rev. **97**, 1279 (1955).
[18] D. C. Oakley and R. L. Walker, Phys. Rev. **97**, 1283 (1955).
[19] Watson, Keck, Tollestrup, and Walker, Phys. Rev. **101**, 1159 (1956).
[20] Corson, Peterson, and McDonald (prepublication summary, 1956). The authors wish to thank Professor D. R. Corson and Professor V. Z. Peterson for communicating these results prior to publication.
[21] K. M. Watson, Phys. Rev. **95**, 228 (1954).

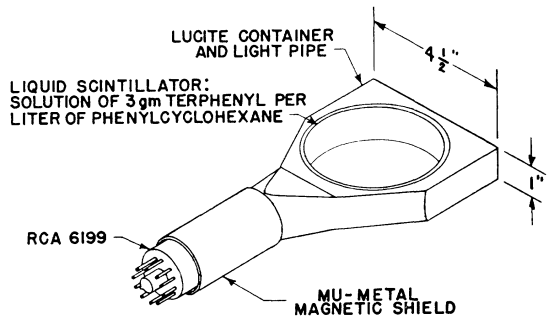

FIG. 1. Liquid scintillation counter unit.

applied here will be described fully in Part II. Borsellino[22] has shown how the single-photon counting rate can be related to the photoproduction angular coefficients. This counting rate at 90° gives a good measure of the total cross section at low energies.

A weak process like the π^0 S-wave does not show up well in the total cross section. It is observed more sensitively through its interference with the much larger P-wave. Again, the angular distribution is difficult to measure at low energies because the photons are emitted practically equally in all directions, and the protons recoiling at large angles have too little energy to be detected. The line of attack pursued here, therefore, is to take some advantage of previous information and to perform two correlated experiments. The first measures the total cross section by counting single photons all the way down to threshold (this means 25 Mev lower than any previous measurement). The second measures the 135° (center-of-mass π^0 angle) differential cross section by observation of recoil protons in emulsions. Here advantage is taken of the facts that the S-P interference is constructive in the backward direction and that these protons recoil at 17.5° in the laboratory, so they can escape a liquid hydrogen target of practical thickness. If the P-wave part of the cross section is fairly well known, the differential cross section at one angle can be compared with the total cross section to obtain the interference

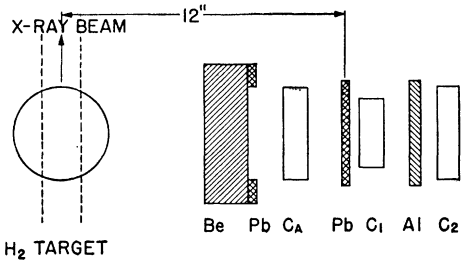

FIG. 2. Geometry for the counter experiment. Scintillators C_1 and C_2 are placed in coincidence, and C_A in anticoincidence. The beryllium block (Be) covers a window in the lead shield (Pb), not shown completely. The lead converter (Pb) was $\frac{1}{4}$ in. thick.

term, and thereby the S-wave, as will be demonstrated in Part III. Unfortunately, however, the P-wave part is not well enough understood to permit a quantitative evaluation of the S-wave in this manner. None of the current theories gives a quantitative prediction of the π^0 S-wave, and more accurate measurements of differential cross sections are necessary to solve this problem.

II. THE COUNTER EXPERIMENT: TOTAL CROSS SECTIONS

A. Apparatus

The process $\gamma+p\rightarrow p+\pi^0$ was observed by detecting one of the γ rays which result from the decay of the π^0. The proton target material was a 4-in.-diameter thin-walled cup of liquid hydrogen surrounded by an aluminum structure which included radiation shields and a vacuum jacket for the hydrogen cup. This target was a modification of the one built by Whalin and Reitz.[23] It supplied 4.21×10^{23} protons per cm^2 in the x-ray beam, and only about 4% of the π^0-decay γ rays were converted to electron pairs in the walls of the target.

The γ rays were detected in a scintillation counter telescope. Each counter was a disk of liquid scintillator (3 grams of p-terphenyl per liter of phenylcyclohexane) enclosed in a Lucite housing which also served as a light pipe. The disks were viewed from the sides by RCA 6199 multiplier phototubes (Fig. 1). Optical contact between the phototube window and the light pipe was made by sealing the two together with Dow Corning 200 fluid.

The mean life of the scintillations was about four millimicroseconds. A typical 6199 tube operating at 1700 volts produced pulses of about 25 ma peak current from passage of a minimum-ionizing particle through the scintillator. The extreme variation in pulse height resulting from scintillations in different parts of the scintillator was 30%.

Figure 2 is a scale drawing of the counting geometry. The target volume was defined by the intersection of the x-ray beam with the cylinder of liquid hydrogen. The amount of irradiation was measured by a thick walled ion chamber 4 meters downstream from the target. True γ-ray counts resulted from the materialization of an electron-positron pair in the lead converter or in counter C_1 and from the passage of either one or both of the pair members through the coincidence counters C_1 and C_2. The anticoincidence counter C_A vetoed counts due to ionizing particles traversing the whole telescope.

The beryllium absorber in front of the telescope reduced the number of ionizing particles entering; thus it helped reduce the counter-jamming. About 4% of the incident γ rays were converted in the beryllium or in counter C_A. The aluminum absorber between C_1 and C_2 eliminated coincidence counts due to low-energy back-

[22] A. Borsellino (private communication to G. Bernardini).

[23] E. A. Whalin and R. A. Reitz, Rev. Sci. Instr. **26**, 59 (1955).

ground radiation. Although this absorber determined an absolute threshold energy for γ-ray detection, the probability for counting such low-energy photons was very small anyway because of the small pair production cross section and the large amount of scattering out of the telescope. In addition to the absorbers shown, the telescope was shielded by four inches of lead and twelve inches of Borax to reduce electron and neutron backgrounds.

Pulses from the counters were analyzed in a fast coincidence-anticoincidence counting system. The phototube current pulse cut off the plate current in a $6AH6$ pentode to produce a pulse of determined height in the plate circuit. The time constant of the grid circuit (dead time) was about 8×10^{-9} second. The length of the signal in the plate circuit was determined by a shorted delay line. These limited and clipped signals were used to operate fast Rossi-type diode coincidence circuits. The resolving time of this combination was 4×10^{-9} second.

Coincidences were taken between C_1 and C_2 and between C_A and C_2. Output signals from these were fed into a diode anticoincidence circuit whose output was then $C_1+C_2-C_A$. This output was amplified and used to fire a fast trigger circuit with a level selector input. Here discrimination against singles and anticoincidences was performed. The trigger circuit output operated a scaler. Figure 3 is a block diagram of the electronic system.

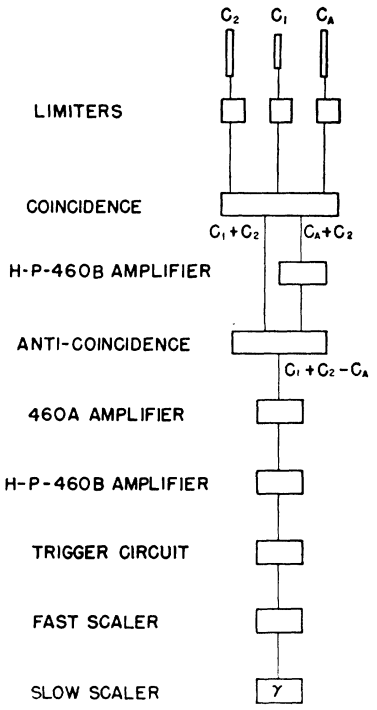

FIG. 3. Block diagram of the electronic equipment.

B. Experimental Procedure

Before useful data could be taken, operating points for the counters and the betatron had to be set for maximum efficiency in counting the desired particles and no others. Most of these settings were established in advance by using the telescope to count penetrating cosmic radiation. In this manner the counters were placed in coincidence, the phototube voltages were set on a plateau, and the discriminators were adjusted to count all coincidences while excluding singles and anticoincidences. Tests performed under actual operating conditions determined the maximum intensity at which the betatron could be operated with negligible effects from accidental coincidences and jamming of the counters. The latter effect was usually the one which limited the useful intensity, if any limitation was necessary. During this testing period, the shielding was developed, and the no-target background was minimized.

To prove that the counts represented γ rays, the counting rate was measured as a function of the lead converter thickness (Fig. 4). The finite counting rate with no converter probably resulted from conversion in the back part of the anticoincidence counter and in the front part of the first coincidence counter. With the addition of more converter, the counting rate increased to a maximum near one radiation length and then slowly decreased. Above the optimum thickness, the number of new pairs produced in additional converter material was smaller than the number of particles removed by scattering or degraded by radiation and ionization in it.

Since a single photon determines neither the angle nor the energy of the meson, other means must be employed. The "photon difference" technique can be used to determine the γ-ray counting rate corresponding to each incident photon energy interval. Then these counting rates are related to suitable parameters of the π^0 angular distributions.

To this end, the net target counting rate at a laboratory angle of 85° was measured as a function of the maximum energy of the bremsstrahlung spectrum. The

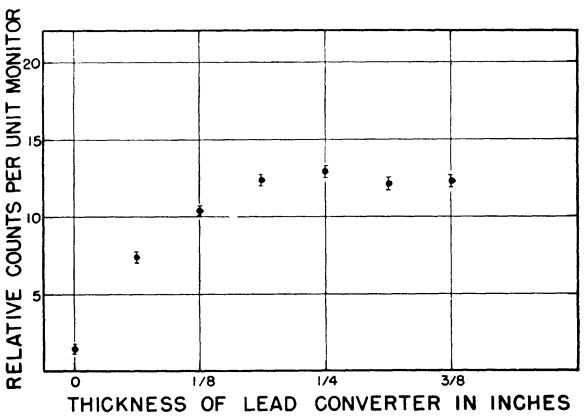

FIG. 4. Counting rate *versus* thickness of lead converter.

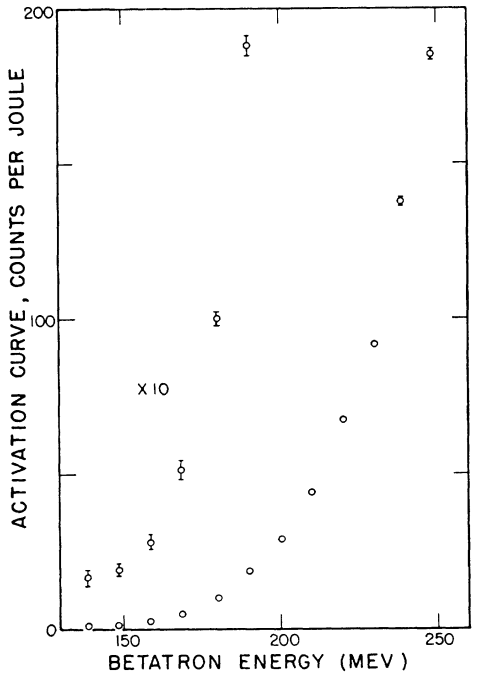

FIG. 5. Counting rate of γ rays from hydrogen at 85°, *versus* betatron energy. Backgrounds with the target evacuated have been subtracted. Indicated errors are standard deviations associated with counting statistics.

betatron energy was varied in 10 Mev steps from 140 Mev, which was below threshold, to 250 Mev. Data were repeated at all energies to avoid instrumental errors. No-target backgrounds varied from half the total counting rate at threshold to 10% of the total counting rate at 250 Mev.

The monitor, a thick-walled ionization chamber, was calibrated against secondary standard ionization chambers, which had been calibrated against a calorimeter.[24] This monitor calibration is considered accurate to 5%. During the experiment, the betatron x-rays were emitted with almost uniform intensity for 500 microseconds at the peak of the 60-cycle sine wave of the magnetic field. The energy spread due to these conditions was 0.5%. The actual energy spread, due to instability of operation, was of the order of 1%. The betatron energy was measured by a flux integration circuit which had been calibrated by magnetic field measurements to an accuracy of 1%.[25]

The net target counting rate as a function of betatron energy is shown in Fig. 5. The extreme concavity of this activation curve makes possible the determination of the slope with reasonable precision even with relatively poor precision in the measurement of the ordinates. This slope is related to the cross section at each point. The fact that the counting rate changes by a factor of 100 between threshold and 250 Mev is ample demonstration that a mesonic process is responsible.

The net counting rate below threshold was shown to be due to γ rays by removing the lead converter. This counting rate was consistent with an elastic scattering cross section with a value half that of the proton Thompson cross section. This background was treated as a constant to be subtracted at all energies. Even if the elastic scattering rose to ten times the Thompson cross section at 250 Mev, it still would be only a 2.5% effect.

C. Analysis of Data

1. Efficiency Calculation

In order to interpret the data, the counter efficiency must be known as a function of γ-ray energy. Not even relative cross sections can be determined without this knowledge, since the spectrum of γ rays from the π^0 decay changes with the meson energy. A Monte Carlo calculation with the aid of the Illiac (University of Illinois Graduate College Computer) is considered the most reliable way to compute the detection efficiency.

The most important parts of this calculation dealt with (1) geometrical effects; (2) pair production in the lead converter, including depth distribution in the lead as well as energy distribution of the pairs; (3) radiation loss by the electrons; (4) multiple scattering of the electrons; and (5) ionization loss by the electrons. An event was started by choosing at random a point in the target where the γ ray originated. Instead of distributing the γ rays uniformly in all directions, time was saved by choosing a point at random on the face of the lead converter. Then, as a weighting factor, the solid angle represented by unit area centered at that point was computed.

The depth at which the pair was produced was chosen on the basis of the exponential depth distribution. Each γ ray was assumed to create a pair, and the weighting factor was just the probability that the corresponding γ ray was converted at all. From this point, the two pair members were followed through the rest of the telescope, their positions and energies being adjusted as they suffered scattering, radiation loss, and ionization loss. If each counter had at least one particle through it, the product of the two weighting factors mentioned above was computed and added to the accumulated weight. This accumulated weight from a large number N of events was then N times the product of efficiency and solid angle of the counter.

The pair production cross sections used were calculated in Born approximation by Aron[26] and corrected to measured pair cross sections quoted by Corson and Hanson.[27] Multiple scattering was treated by assuming a Gaussian distribution of scattering angles with the

[24] P. D. Edwards and D. W. Kerst, Rev. Sci. Instr. 24, 490 (1953).
[25] T. B. Elfe and F. Ore (unpublished).
[26] W. A. Aron (private communication to D. W. Kerst).
[27] D. R. Corson and A. O. Hanson, *Annual Review of Nuclear Science* (Annual Reviews, Inc., Stanford University, 1953), Vol. 3, p. 67.

same $1/e$ width as that predicted by the Molière theory.[28] This treatment has been shown to give good agreement with measurements of multiple scattering.[29] Bethe-Heitler radiation probability functions[30] were used to describe the radiation loss of the electrons. Since the radiation straggling distribution was a strong function of the radiator thickness, it was necessary to store distributions corresponding to several thicknesses and to interpolate between these in an actual event. The Landau[31,32] distribution of ionization losses, with the most probable energy loss given by the Landau formula with density correction, was used to describe the ionization energy losses of the electrons.

In addition to the Monte Carlo evaluation, the reduction in efficiency owing to conversion in materials preceding the telescope and in the anticoincidence counter was also considered. This correction amounted to about 5% at the lowest energy and about 10% at the highest energy.

The results are shown in Fig. 6. Indicated errors are statistical in nature. Usually, enough events were followed to yield about 1000 successful tracks, with a statistical error of about 3%. The calculation was repeated at 155 Mev with different sets of random numbers to check the reliability of the method. Pair production cross section measurements[27] showed probable errors of about 4%. Errors introduced by approximations, interpolations, and uncertainties in physical cross sections combined with the statistical uncertainty mentioned above to yield a probable error of 6% in the absolute value of the efficiency.

2. *Relation between γ-Ray Counts and π^0 Photoproduction Cross Sections*

In its own rest frame, the π^0 decays isotropically into two photons, each of energy $\mu c^2/2$. The Lorentz transformation from this frame to the photoproduction center-of-mass system results in a unique relation between the energy of the photon and the angle between meson and photon directions. For γ rays emitted in a certain direction in the center-of-mass system, an integration over all π^0 directions is equivalent to an integration over the γ-ray energy spectrum, since the π^0 energy is independent of angle in this system.

This γ-ray energy spectrum will, of course, depend on the angular distribution of the pions. If the photoproduction cross section can be expressed as

$$\sigma_\pi(\theta_\pi)=A+B\cos\theta_\pi+C\cos^2\theta_\pi, \tag{2}$$

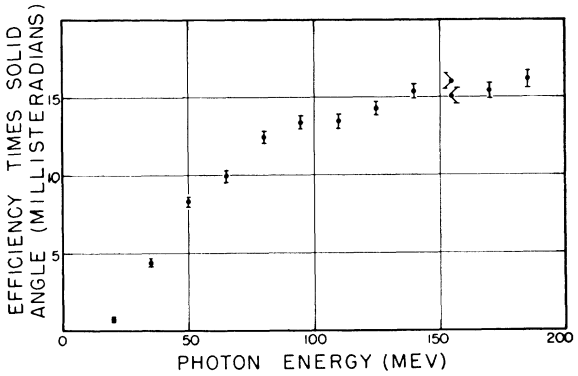

FIG. 6. Counter efficiency times solid angle *versus* γ-ray energy, as calculated by the Monte Carlo method described in the text.

then the γ-ray counting rate per proton per unit of incident γ-ray flux is

$$I(\theta_\gamma)=\alpha(A+hB+gC), \tag{3}$$

where

$$\alpha=\frac{2}{q}\int_{k_{\min}}^{k_{\max}}\eta\Omega(k)dk \tag{4}$$

is twice the average efficiency times solid angle of the telescope in the interval of photon energies present in the spectrum, since $k_{\max}-k_{\min}=q$. Here k is the photon momentum, and q is the π^0 momentum. The efficiency times solid angle, $\eta\Omega(k)$, is here defined in the center-of-mass system by means of a simple transformation. The quantities

$$h=(\beta\cos\theta_\gamma)/\alpha \tag{5}$$

and

$$g=[\alpha-\gamma+(3\gamma-\alpha)\cos^2\theta_\gamma]/2\alpha \tag{6}$$

are referred to as dynamical efficiencies, where

$$\beta=\frac{2}{q}\int_{k_{\min}}^{k_{\max}}(\cos\theta)\eta\Omega(k)dk, \tag{7}$$

$$\gamma=\frac{2}{q}\int_{k_{\min}}^{k_{\max}}(\cos^2\theta)\eta\Omega(k)dk, \tag{8}$$

θ is the angle between meson and decay photon directions, and θ_γ is the colatitude angle of the γ ray in the center-of-mass system.

The integrands involved in α, β, and γ are plotted and integrated graphically. The resulting values for α, h, and g are given in Table I. A useful quantity is the effective γ-ray cross section,

$$\sigma'(\theta_\gamma)=I(\theta_\gamma)/\alpha=A+hB+gC, \tag{9}$$

which permits an intuitive understanding of the variation of h and g with energy. For incident photon energies near threshold, the π^0 moves so slowly that the decay photons appear almost isotropically. Then h vanishes, and g approaches $\frac{1}{3}$, so that σ' is a sample of the total

[28] G. Molière, Z. Naturforsch. **3a**, 78 (1948); **2a**, 133 (1947).
[29] Hanson, Lanzl, Lyman, and Scott, Phys. Rev. **84**, 634 (1951).
[30] H. Bethe and W. Heitler, Proc. Roy. Soc. (London) **146**, 83 (1934).
[31] J. Landau, J. Phys. U.S.S.R. **8**, 201 (1944).
[32] R. M. Sternheimer, Phys. Rev. **88**, 851 (1952); Goldwasser, Mills, and Hanson, Phys. Rev. **88**, 1137 (1952).

TABLE I. Values of detector efficiency times solid angle (α) and dynamical efficiencies (h and g) averaged over the decay photon energy spectrum for various incident photon energies (E).

E, Mev	α, sterad	h	g
150	0.02212	−0.0149	0.321
160	0.02232	−0.0270	0.300
170	0.02270	−0.0367	0.283
180	0.02276	−0.0460	0.268
190	0.02330	−0.0539	0.253
200	0.02340	−0.0606	0.243
210	0.02354	−0.0710	0.229
220	0.02354	−0.0762	0.220
230	0.02410	−0.0851	0.216
240	0.02396	−0.0944	0.205
250	0.02406	−0.1022	0.190

cross section,

$$\sigma_T = 4\pi(A+\tfrac{1}{3}C). \tag{10}$$

At high energies, h approaches $\cos\theta_\pi$, and g approaches $\cos^2\theta_\pi$.

One should note that the quantities in this section are related to a unique incident photon energy. The method of determining the yield $I(\theta_\gamma)$ corresponding to a certain incident photon energy will be described in the next section.

3. *Analysis of the Activation Curve*

In order to determine the actual cross sections as a function of incident photon energy from the measured activation curve, an integral equation relating the two quantities must be solved. Since the activation curve is measured at a discrete set of points, approximate numerical solutions to the problem must be sought. Several methods have been proposed.[33–35] The method applied here is that of Leiss and Penfold,[35] which, in most instances, gives the same solution as that obtained by Katz and Cameron.[33]

The nature of this solution is as follows: Let the activation curve be measured at equally spaced betatron energies $E_{0n}=E_t+(n-1)\Delta$, where Δ is the spacing between energies, E_t is the threshold for the process, and n is an integer. Let the spectrum $P(E_0,E)$ at energy E_{0n} be $P_n(E)$. Then

$$A_n=\int_0^{E_{0n}} P_n(E)\sigma(E)dE, \tag{11}$$

where $\sigma(E)$ is the cross section. Multiply A_n by a set of coefficients B_{mn}, as yet unspecified, and sum over n. Then

$$\sum_n B_{mn}A_n=\int_0^{E_n} T_m(E)\sigma(E)dE, \tag{12}$$

where the "weighting function" $T_m(E)$ is given by $T_m(E)=\sum_n B_{mn}P_n(E)$. This function must be chosen such that the integral involving $T_m(E)$ is approximately the cross section in the mth energy interval. The choice of Leiss and Penfold is to make $T_m(E)$ identically zero throughout all energy intervals above the mth, and equal to zero at the center of each interval below the mth. The value of $T_m(E)$ in the mth interval is taken to be $P_m(E)/P_{mm}\Delta$, where P_{mm} is the value of $P_m(E)$ at the center of the mth interval. This set of conditions uniquely determines the coefficients B_{mn}. The approximation to the cross section at the center of the mth interval is

$$\sigma(E_m-\Delta/2)=\sum_{n=0}^{m} B_{mn}A_n. \tag{13}$$

The bremsstrahlung spectrum emitted by the betatron has been measured by Leiss, Hanson, and Yamagata[36] and has been shown to agree with the zero degree thin target spectrum of Schiff[37] with the constant $C=191$. These spectra, therefore, have been used to compute the coefficients B_{mn} with the aid of the Illiac.

D. Experimental Results

The counting rates presented in Fig. 5 were measured at unequal energy intervals. In order to apply the

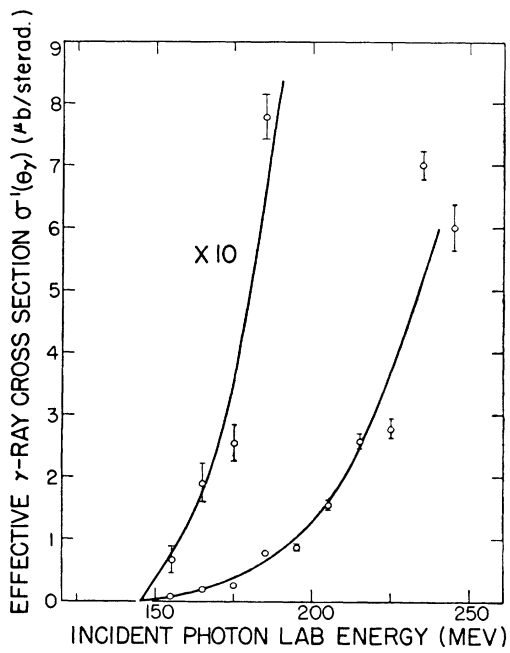

FIG. 7. Effective γ-ray cross section $\sigma'(\theta_\gamma)$ *versus* laboratory energy of the incident photon. The solid curve results from application of the photon difference analysis to a smooth curve through the points of Fig. 5. Application without smoothing leads to the points shown here. Indicated errors arise from counting statistics.

[33] L. Katz and A. G. W. Cameron, Can. J. Phys. **29**, 518 (1951).
[34] L. V. Spencer, National Bureau of Standards Report No. 1531, 1952 (unpublished).
[35] J. Leiss and A. S. Penfold (to be published).
[36] J. Leiss, Ph.D. thesis, University of Illinois, 1954 (unpublished).
[37] L. I. Schiff, Phys. Rev. **83**, 252 (1951).

photon difference analysis outlined above, a curve was drawn through these points, and values were taken from the curve at 5-Mev intervals. The resulting yield as a function of incident photon energy, when divided by the number of protons/cm^2 in the target and by the average counting efficiency times solid angle (α), gave the effective γ-ray cross section $\sigma'(\theta_\gamma)$ shown by the solid curve of Fig. 7. The points on this figure were obtained from a separate evaluation in which the measured counting rates were analyzed without any smoothing. Then the indicated errors were simply computed by the usual rule for propagation of errors, in which only standard deviations in the counting statistics were included.

An error in the betatron energy has an exaggerated effect on these points because the number of incident photons depends on the difference between successive machine energies. Since each measured counting rate is used repeatedly, a low point on Fig. 7 is immediately followed by a high point, and vice versa. Not to smooth the activation curve is to discard the assumption that the cross section is smooth. For this reason, the solid curve of Fig. 7 is considered the best representation of the results of this experiment.

The effective γ-ray cross section, $\sigma'(\theta_\gamma)$, has been shown to approach the ordinary total cross section divided by 4π at energies near threshold. Because the asymmetric term hB is vanishingly small in these measurements near 90°, the total cross sections can be deduced from $\sigma'(\theta_\gamma)$ at each energy by inserting the

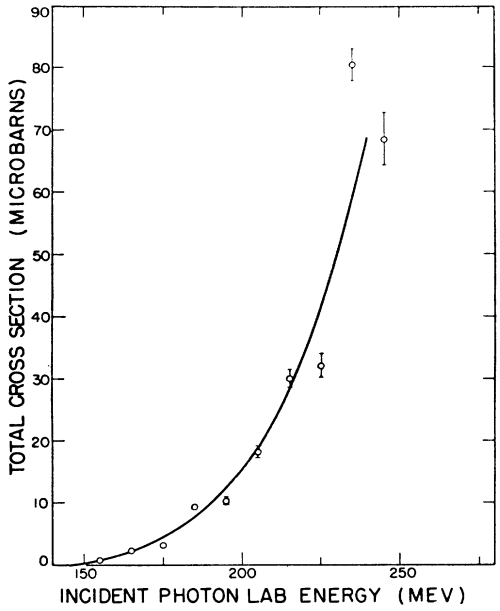

FIG. 8. Total cross sections for photoproduction of π^0 mesons in hydrogen, in units of 10^{-30} cm^2. The solid curve and the points are derived, respectively, from the solid curve and from the points of Fig. 7.

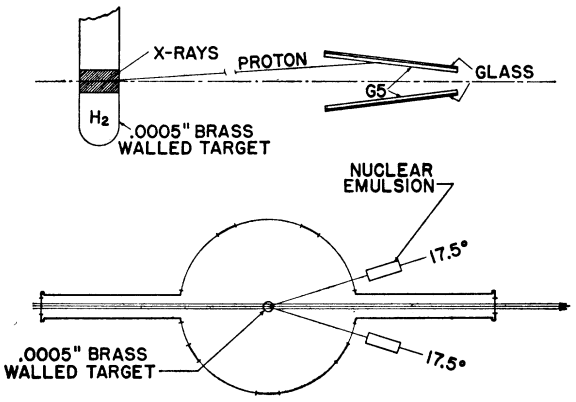

FIG. 9. Schematic diagram of liquid hydrogen target and nuclear emulsion detectors.

value of C/A in the relation

$$\sigma_T = 4\pi\sigma'(\theta_\gamma)[1+C/3A]/[1+gC/A]. \quad (14)$$

The value -0.6 was chosen for C/A on the basis of other experiments. Because the function g has a value near $\frac{1}{3}$ at all energies involved in this experiment, the total cross sections obtained in this manner are very insensitive to the assumed value of C/A. In particular, changing C/A from -0.6 to -1.0 changes σ_T by 10% at 240 Mev and by successively smaller percentages at the lower energies.

Figure 8 shows the total cross sections derived from the values of $\sigma'(\theta_\gamma)$ on Fig. 7 by means of (14). In addition to statistical deviations in the counting rates, errors in the absolute cross section arise from the 6% uncertainty in the efficiency calculation and from the 5% uncertainty in the x-ray monitor. These errors, then, contribute an additional 8% uncertainty in the absolute cross section. Finally, the absolute energy of the betatron may be systematically in error by 1%.

III. EMULSION EXPERIMENT

A. Apparatus

Observation of the recoil protons in nuclear emulsions provides a direct measurement of the absolute differential cross sections. The incident photon energy and the center-of-mass angle are uniquely related to the energy and angle of the recoil proton.

Goldschmidt-Clermont *et al.*[16] used this method with a high pressure gas target. The present experiment differs from theirs in that the target volume is defined by the intersection of the x-ray beam with the cylinder of liquid hydrogen (Fig. 9), and the recoil angle is determined by the position of the emulsion.

The liquid hydrogen target,[23] beam collimation, and ionization chamber monitor[24] were the same as those used by Bernardini and Goldwasser,[38] except that the

[38] G. Bernardini and E. L. Goldwasser, Phys. Rev. **94**, 729 (1954); Beneventano, Bernardini, Lee, Stoppini, and Tau, Nuovo cimento **4**, 323 (1956).

diameter of the liquid hydrogen appendix was reduced to $\frac{7}{8}$ in. Each detector consisted of two pellicles clamped to a plate to form a stack of emulsion 1.8 mm thick and 1 inch×3 inches in area. These fitted into milled grooves in the Bakelite boxes designed by Reitz,[39] so that the emulsion surface was fixed at 7° from the horizontal plane. Each stack was marked with four x-ray pencils to permit following of tracks from one pellicle to the next. The exposed pellicles were stuck to glass plates prior to development; thereafter they had all the properties of ordinary plates.

Ilford G-5 emulsions, which are sensitive to minimum ionizing particles, were chosen for this experiment for several reasons. First, the darkness of the proton tracks made surface scanning efficient. Second, the high electron background appeared as distinguishable tracks rather than as a general fog. Finally, this type of emulsion had been used extensively at this laboratory and had been found very uniform.

The electron background was strongly reduced by underdeveloping the emulsions at 15°C for 40 minutes with 30% water and 8 cc per liter of 10% KBr added to the normal amidol developer.[40] Pellicles that received a dosage of 300 mr were transparent, while proton tracks up to 70 Mev were clearly visible in them. The highest proton energy of interest was less than 45 Mev.

B. Procedure

During the exposure, the betatron was operated at an energy of 225 Mev. The line connecting target and emulsion centers made an angle of 17.5° with the x-ray beam. Tolerable exposures permitted about 175 useful tracks per emulsion with the target full and about 110 with the target evacuated. Altogether, the number of tracks measured was about 2500.

These tracks were found by scanning the surface of the emulsion for tracks entering from the direction of the target. To check the efficiency, three stacks were scanned twice by different scanners using the same microscope. Out of 446 tracks correlated in this manner, only 5 new ones were found, and these did not fall in any particular energy range. Thus the scanning efficiency is considered better than 98%.

The proton energies were determined by their ranges,[41,42] which varied from 0.7 to 6.3 mm for acceptable tracks. The ranges were measured in terms of initial and final coordinates in each layer of the stack and of coordinates of scatterings in the emulsion. Positive identification of the protons was no problem. Only about one track per thousand penetrated through the emulsion stack with a visible range less than 6.3 mm. The residual energy was then estimated on the basis of grain density.

Fading in the emulsion surface made the first 0.1 mm of track hard to see. A correction to the range was applied by measuring the dip angle of each track and projecting backward to the surface of the emulsion. Range errors of the order of 0.1 mm arose from this effect. Because the protons traversed an equivalent of 0.304 g/cm² of aluminum windows between the target and the emulsion, an error of 0.1 mm on the range measurement caused an error of at most 1 Mev on the determination of the incident photon energy. The continuous spectrum of proton energies also reduced errors due to indefinition of range band limits. Tracks spilling out of a band were compensated by other tracks spilling in.

The tracks in the emulsions exposed to the liquid hydrogen target included a substantial number of photoprotons from the 0.0005-in. brass wall containing the hydrogen (about 50% at 180 Mev and 25% at 210 Mev). These protons were measured in a separate exposure with the container evacuated and were subtracted.

C. Analysis of Data

The center-of-mass differential cross section for photoproduction of π^0 mesons at angle θ^* by photons of energy E is

$$\frac{d\sigma}{d\Omega^*}(E,\theta^*)=\frac{Y}{[NQ\Omega(d\Omega^*/d\Omega)]}, \tag{15}$$

where Y is the number of protons counted, N is the number of target atoms/cm², Q is the number of incident photons in the energy interval $E\pm\Delta E$, Ω is the laboratory solid angle, and $d\Omega^*/d\Omega$ is the center-of-mass to laboratory solid angle ratio.

The number $N=0.892\times10^{23}$ atoms/cm² was computed from the molar volume of liquid hydrogen under the experimental conditions[43] and the volume of the intersecting cylinders divided by the beam area. Variations in the beam intensity over its area were negligible.

The solid angle Ω is calculated by a straightforward integration along the scanned portion of each emulsion, in which variation across the 1.3-cm width is neglected. The solid angle is directly proportional to the 7° tilt angle, which may be in error by something less than 5% because of play in the milled grooves. The method of exposing above and below the beam level compensates for a misalignment of the box as a whole. The results of pairs of emulsions agree within their statistical deviations, but in cases of systematic differences the dip angle distributions of the tracks roughly confirm the differences in solid angle.

The number Q is computed from bremsstrahlung tables.[35] That the average photon energy occurs at the center of the interval can be shown by integrating the

[39] R. A. Reitz, Ph.D. thesis, University of Illinois, 1955 (unpublished).
[40] A. Beiser, Revs. Modern Phys. **24**, 273 (1952).
[41] J. J. Wilkins, Atomic Energy Research Establishment Report, Harwell AERE-*G/R* 664, 1951 (unpublished).
[42] M. Rich and R. Madey, University of California Radiation Laboratory Report UCRL-2301, 1954 (unpublished).
[43] Wooley, Scott, and Brickwedde, J. Research Natl. Bur. Standards **41**, 379 (1948).

TABLE II. Center-of-mass differential cross sections in units of 10^{-30} cm²/steradian.

Laboratory photon energy (Mev)	Target full		Target evacuated		Normalized net yield	c.m. π^0 angle	Differential cross section
	Total tracks	Normalized yield	Total tracks	Normalized yield			
180±5	487	8.10	196	4.41	3.69	130°±7°	0.99±0.13
190±5	407	6.77	123	2.77	4.00	133°±7°	1.30±0.14
200±5	454	7.56	125	2.82	4.74	135°±6°	1.78±0.16
210±5	431	7.17	83	1.87	5.30	136°±6°	2.32±0.18
215±5	311	5.74	75	1.69	4.05	137°±6°	2.00±0.19

product of photon energy, laboratory cross section, and bremsstrahlung spectrum over the interval. For photon energies between 180 and 215 Mev and for 10-Mev intervals, the average value lies within 0.2 Mev of the median energy.

The primary consideration in the choice of energy intervals is the uncertainty in the energy lost by the proton in the hydrogen target itself. A given residual range in the emulsion corresponds to incident photon energies spread over a 10- to 15-Mev interval.

A preliminary step in the analysis was to calculate the distribution of proton path lengths in the hydrogen. The simplest way to perform this calculation was by means of a Monte Carlo method with the Illinois digital computer.[44]

The average energy of the incident photons which produce protons of range R in the emulsion is

$$\langle E\rangle=\int_0^{2.22\text{ cm}} E_l P_l Q(E_l)\frac{d\sigma}{d\Omega}(E_l)dl \Big/ \int_0^{2.22\text{ cm}} P_l Q(E_l)\frac{d\sigma}{d\Omega}(E_l)dl, \quad (16)$$

where E_l is the photon energy necessary to produce a proton of residual range R after traversing the hydrogen thickness l, P_l is the ordinate of the path length distribution at l, $Q(E_l)$ is the bremsstrahlung ordinate at E_l, and $d\sigma/d\Omega(E_l)$ is the laboratory cross section at E_l. The resulting value of $\langle E\rangle$ is always within 1% of the photon energy corresponding to a proton which traverses the average path length in the hydrogen. A one-to-one correspondence between ranges and energies is set up in this manner. The band of incident photon energies, centered at the nominal energy, is chosen 10 Mev wide and determines the band of ranges.

A simple correction for energy losses in the hydrogen was applied to the protons ejected from the thin brass walls. Since half of the wall protons passed through the hydrogen, the emulsion equivalent of the hydrogen was subtracted from the ranges of half of the tracks observed with the target evacuated. This procedure necessitated the recording of wall protons up to 7.6-mm range in the emulsion instead of 6.3 mm. About 25% of the protons in this last range interval penetrated through the emulsion, so their energies are less certain than those of the slower protons.

The angular interval of the recoil protons as defined by the boundaries of target and emulsions is 17.5° ±2.5°, including small angle scattering in the hydrogen and in the windows. This angular spread is confirmed by the measured entrance angles. The corresponding π^0 center-of-mass angular range is approximately 135°±6°. This angular uncertainty leads to an uncertainty of 3 Mev in the incident photon energy[45] as determined by the proton range. This error is overshadowed by the energy losses of protons in the hydrogen.

Table II summarizes the results of the experiment. The differential cross sections are given at the center-of-mass π^0 angle corresponding to the 17.5° laboratory proton angle for each energy. The differences between these values and those of the 135° cross sections are smaller than the experimental errors both in this measurement and in the angular distributions. In the concluding discussions, therefore, these tabulated values will be taken as 135° cross sections.

D. Summary of Errors

The standard deviations on the numbers of protons observed comprised the largest error (10%) in this experiment. Other errors included 5% on the solid angle and 4% on the beam monitor. The scanning efficiency was checked at better than 98% as described above, and no correction was applied. The number of target atoms/cm² is considered known to better than 1%. The measurement of the betatron x-ray spectrum by Leiss, Yamagata, and Hanson[36] agreed, within the precision of the apparatus, with a spectrum of the type assumed above.

No correction is applied for protons recoiling from the elastic scattering of photons. This effect is probably less than 5% for these energies.[46] The above errors combine to a total of from 12 to 15% between 180 and 210 Mev.

Two additional errors apply to the 215-Mev point. A shift of the betatron energy downward by 2.5 Mev (slightly more than 1%) changes the number of photons in the interval 210–220 Mev by about 10%. The error

[44] This problem was coded by E. A. Whalin, Ph.D. thesis, University of Illinois, 1954 (unpublished), p. 24.

[45] J. H. Malmberg and L. J. Koester, Jr., "Tables of nuclear reaction kinematics at relativistic energies," University of Illinois, 1953 (unpublished).

[46] T. Yamagata (private communication).

in the energy calibration is about $\pm 1\%$.[25] Since about 30% of the protons in this band come from the walls, the 25% which penetrate through the emulsion represent only 7% of the entire group. Probably less than half of these are subtracted erroneously. Thus the overall error for the 215-Mev point is about 17%.

IV. CONCLUSIONS

A. Relation between Photoproduction and Scattering of π^0 Mesons

The total cross sections measured in this experiment can be compared with scattering cross sections in a way that involves very little analysis.[47] Because the neutral pions are produced mainly by magnetic dipole interaction through the $(\frac{3}{2},\frac{3}{2})$ state, the most important part of the photoproduction matrix element, as given by the Chew-Low theory,[13] is

$$\mathcal{H}_k{}^v(q)=-\frac{1}{f_r}\left(\frac{\mu_p-\mu_n}{2}\right)\frac{F(k^2)}{v(k)}\left(\frac{\omega_p}{k}\right)^{\frac{1}{2}}T_p(q), \quad (17)$$

where f_r^2 is the rationalized, renormalized coupling constant, μ_p, μ_n are the nucleon magnetic moments, $F(k^2)$ is a form factor (taken equal to unity here), $v(k)$ is the cutoff function (also equal to unity here), ω_p is the total energy of a meson of type p, in units of μc^2, k is the incident photon energy or momentum, and $T_p(q)$ is the matrix element for pion scattering from the state p to the state q.

This simple relation between the photoproduction and scattering of π^0 mesons does not arise merely from the general theory of scattering but rather from the particular way in which the current density operator $\mathbf{j}$ is divided.[48] The first two terms in $\mathbf{j}$, namely $\mathbf{j}_v+\mathbf{j}_s$, have the same matrix elements as $\mathbf{j}$ itself between single physical nucleon states. The third term, $\mathbf{j}_\pi$, which is not the conventional meson current operator, has no overlap between these states but affects only the excited states. This procedure emphasizes the role of the static nucleon in the absorption of the incident photon and makes possible the use of physical nucleon properties such as the magnetic moments in the photoproduction matrix elements.

The total cross section resulting from the matrix element (17) is

$$\sigma_{TP}{}^{\gamma 0}=C\left(\frac{\mu_p-\mu_n}{2}\right)^2\frac{1}{f_r^2}\frac{\omega_p}{k}|T_p(q)|^2, \quad (18)$$

where $\hbar=c=1$, the superscripts $\gamma 0$ refer to neutral photoproduction, the subscripts TP refer to total P-wave cross section, energies are measured in units of the meson rest mass, and

$$C=\frac{q\omega_q}{(2\pi)^2(1+k/M)(1+\omega/M)}\approx\frac{q\omega_q}{(2\pi)^2(1+\omega/M)^2}$$

involves the incident flux and density of final states. Actually, the factors $(1+\omega/M)(1+k/M)$ are included implicitly in the form of $T_p(q)$ that is used in practice, but they can be written this way with a different $T_p(q)$ understood.

For the scattering of P-wave neutral mesons of momentum q_0, the total cross section is[13]

$$\sigma_{TP}{}^{00}=C|T_{q0}(q)|^2/v_\pi, \quad (19)$$

where $v_\pi=q_0/\omega_{q0}$ is the velocity of the incident pion. The matrix elements in (18) and (19) can be brought into the same form by means of the relation

$$|T_p(q)|^2=\left|\left(\frac{\omega_q}{\omega_p}\right)^{\frac{1}{2}}\frac{\mathbf{p}}{q_0}T_{q0}(q)\right|^2, \quad (20)$$

where $\mathbf{q}_0$ is a vector of magnitude q_0 and direction $\mathbf{p}/p=\mathbf{k}\times\boldsymbol{\varepsilon}/|\mathbf{k}\times\boldsymbol{\varepsilon}|$. Then the photoproduction cross section becomes

$$\sigma_{TP}{}^{\gamma 0}=C\left(\frac{\mu_p-\mu_n}{2}\right)^2\frac{1}{f_r^2}\frac{\omega_q}{k}\frac{p^2}{q_0{}^2}|T_{q0}(q)|^2$$
$$\approx C\left(\frac{\mu_p-\mu_n}{2}\right)^2\frac{1}{f_r^2}\frac{1}{v_\pi{}^2}|T_{q0}(q)|^2, \quad (21)$$

since $k\approx\omega_{q0}$ and $p^2=k^2$.

The ratio of the cross sections is thus

$$\sigma_{TP}{}^{\gamma 0}/\sigma_{TP}{}^{00}=(\mu_p-\mu_n)^2/4f_r^2v_\pi=0.0026/v_\pi \quad (22)$$

for an unrationalized coupling constant $f^2=f_r^2/4\pi=0.081$.

The π^0 scattering cross sections may be obtained from those of the charged pions by the consequence of charge independence. The relation is

$$\sigma^{00}=(\sigma^{++}+\sigma^{--}-\sigma^{-0})/2, \quad (23)$$

where the superscripts on the right refer, respectively, to the processes

$$\pi^++p\rightarrow\pi^++p,$$
$$\pi^-+p\rightarrow\pi^-+p,$$
$$\pi^-+p\rightarrow\pi^0+n.$$

Figure 10 shows cross sections for these processes published in the literature.[8] The operation (23) is performed on the curves drawn rather arbitrarily through the points. This subtraction magnifies the statistical errors, but not prohibitively, since σ^{++} is substantially larger than σ^{-0}.

The S-wave part of π^0 scattering, again by charge

[47] The authors wish to thank Professor T. D. Lee and Professor G. F. Chew for suggesting this comparison.

[48] See reference 13, page 1580. A derivation of relation (17) is given on the same page.

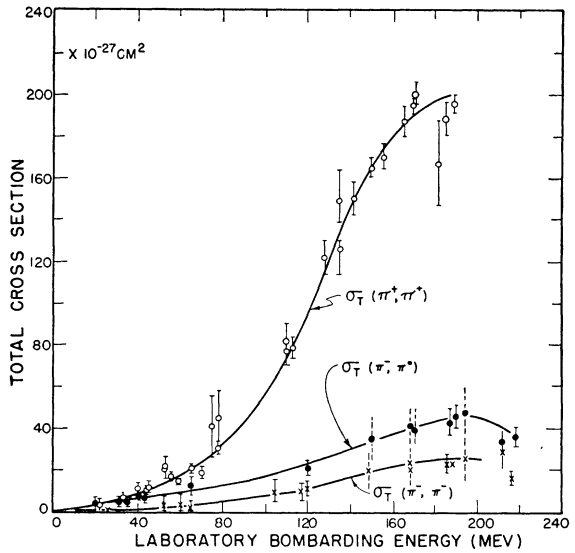

FIG. 10. Published values of total cross sections for pion-proton scattering *versus* laboratory kinetic energy of the incident pion. See reference 8 for a bibliography.

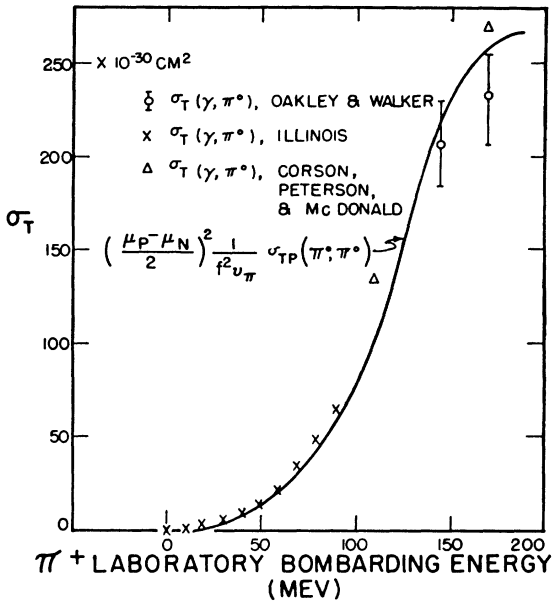

FIG. 11. The relation between π^0 photoproduction and scattering at the same total energy in the center-of-mass system. Abscissas are laboratory kinetic energies of incident charged pions. The solid curve is derived from the scattering cross sections of Fig. 10 by means of relations (22)–(24), while the points represent measured photoproduction cross sections.

independence, is

$$\sigma_{TS}{}^0 = (4\pi\lambda^2/9) \times\{6\sin^2\alpha_3+3\sin^2\alpha_1-2\sin^2(\alpha_1-\alpha_3)\}, \quad (24)$$

where α_1 and α_3 are the S-wave scattering phase shifts corresponding to isotopic spin states $\frac{1}{2}$ and $\frac{3}{2}$, respectively. This is the only point at which the phase shift analyses influence the results of this section, and this influence is very small because $\sigma_{TS}{}^{00} \ll \sigma_{TP}{}^{00}$.

The demonstration of relation (22) appears in Fig. 11. Here the solid curve is $0.0026\sigma_{TP}{}^{00}/v_\pi$, and the points are measured values of $\sigma_T{}^{\gamma 0}$. The neutral photopion S-wave is not subtracted because its magnitude is uncertain and is of the order of the statistical deviations. This comparison between the two cross sections is made at the same value of the total energy in the center-of-mass system. This means that if the laboratory kinetic energy of the incident π^+ meson is T_{π^+}, then the laboratory energy of the incident photon E_γ must be

$$E_\gamma = T_{\pi^+} + 150.1 \text{ Mev}. \quad (25)$$

One should note that the agreement exhibited in Fig. 11 does not rule out a reasonably small electric quadrupole contribution to the photoproduction, which would appear in the differential cross sections as a more negative value of C/A in (2) but not in these total cross sections. The results of Corson, Peterson, and McDonald,[20] however, indicate that the electric quadrupole contribution is indeed very small.

B. Implications of the Differential Cross Sections

The two experiments described above were performed on the assumption that the symmetric part of the angular distribution was fairly well established. In other words, in the expression (2), the ratio C/A was believed to have a value near -0.6 at all energies below resonance. In such a case, a measurement of $\sigma_T = 4\pi \times (A+\frac{1}{3}C)$ would provide values for both A and C which could be substituted into (2). Then subtraction from the differential cross section measured at one angle would yield B.

When this procedure is followed, however, the values of the 135° differential cross sections measured by the proton recoils are so large as to imply negative cross sections at zero degrees. Unless one of the two experiments is seriously in error, the magnitude of C/A must decrease at low energies. A lower limit on the amount of this decrease in magnitude can be illustrated by finding the most negative values of C/A consistent with these two experiments, i.e., the values for which $\sigma(\theta=0)=0$.

The total cross section values quoted above may be used here, but instead the effective γ-ray cross sections $\sigma'(\theta_\gamma)$ (Fig. 7) will be used because they are closely related to the total cross sections, are directly observed, and involve no assumptions regarding the value of C/A.

The three simultaneous equations to be satisfied are

$$A+B+C=0, \quad (26a)$$

$$A-0.707B+0.5C=d\sigma(135°)/d\Omega^*, \quad (26b)$$

$$A+hB+gC=\sigma'(85°), \quad (26c)$$

where g and h are the dynamical efficiencies defined by (5) and (6), $d\sigma(135°)/d\Omega^*$ is the differential cross sec-

TABLE III. Energy variation of the lower limit placed on the value of C/A by this experiment. Cross sections are given in units of 10^{-30} cm²/steradian.

1 Incident photon energy Mev	2 Effective γ-ray cross section $\sigma'(\theta_\gamma)$	3 Differential cross section $\sigma(135°)$	4 C/A (min) for mean values of $\sigma'(\theta_\gamma)$, $\sigma(135°)$	5 C/A (min) at standard deviations	6 C/A for $B=0$ at standard deviations	7 C/A Chew and Low theory
180	0.494±0.05	0.99±0.13	+0.67	−0.075	+7.6	+0.036
190	0.837±0.071	1.30±0.14	−0.095	−0.44	+1.6	−0.080
200	1.28 ±0.12	1.78±0.16	−0.29	−0.56	+0.72	−0.188
210	1.99 ±0.16	2.32±0.18	−0.54	−0.71	−0.02	−0.279

tion measured in the emulsion experiment, and $\sigma'(85°)$ is the effective γ-ray cross section measured in the counter experiment. Equation (26a) expresses the limiting condition here. The solutions of (26) for C/A are listed in Table III for four energies of observation (Column 4). To show how much latitude is allowed by the counting statistics, the values at the statistical deviation of each experiment in the direction which makes C/A more negative are inserted for the solutions listed in Column 5. The value -0.6 is seen to be consistently outside the standard deviations up to 200 Mev.

The energy dependence of C/A suggested by Column 4 appears very naturally in the theories of Chew and Low[13,49] and of Ross.[50] It arises from the interference between enhanced and unenhanced P-states alone and has no connection with the S-wave. This P-state interference yields a monotonic decrease in C/A from small positive values near threshold to about -0.6 at resonance.

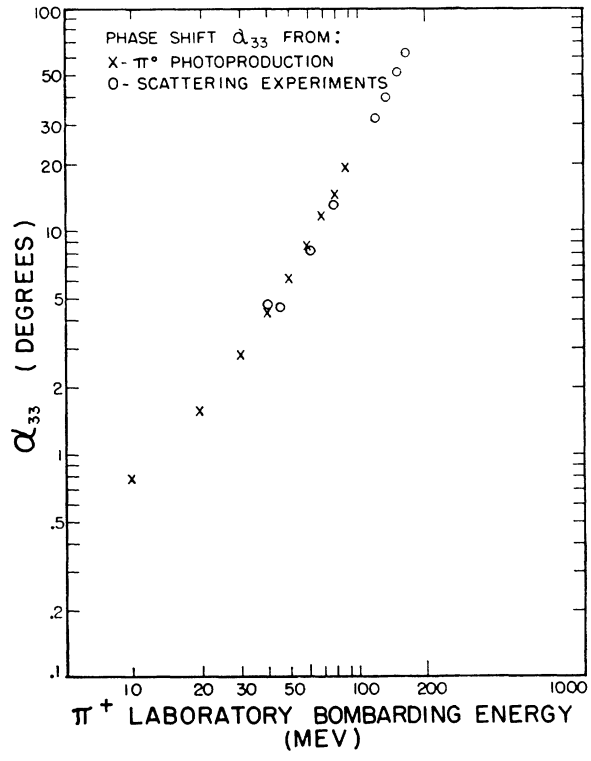

FIG. 12. Values of the phase shift α_{33} derived from π^0 photoproduction by means of relation (30), compared with values measured in π-p scattering experiments. For convenience, the abscissas are the laboratory kinetic energies of incident charged pions.

The S-state production is apparent only in the asymmetric part of the angular distribution. Since the pseudoscalar nature of the pions requires an electric dipole interaction for S-state production, a neutral photopion S-wave must arise from nucleon recoil or from internal rescattering of S-state charged pions. Both of these effects are small and, except at energies very near threshold, contribute to the cross section only through interference with the dominant P-wave. This interference is represented by the term $B\cos\theta$ in the angular distribution.

Although the present experiments are inadequate to provide quantitative information regarding the S-wave. they do indicate the existence of a finite amount of S-state production. In Eqs. (26), if $B=0$, then (26b) and (26c) must be satisfied subject to the inequalities $A+C\geq 0$ and $A\geq 0$. The resulting values of C/A are listed in Column 6 of Table III. Here again, to be conservative, the cross sections at the standard deviations in the direction to minimize C/A are inserted. In the absence of constructive S-P interference at 135°, the angular distribution must have a substantial dip at 90°, in contradiction to all current theories.

If only the nucleon recoil contributed to S-state production, the interference term would be proportional to $\sin\alpha_{33}\cos\alpha_{33}$, where α_{33} is the scattering phase shift corresponding to the state of isotopic spin $\frac{3}{2}$ and angular momentum $\frac{3}{2}$. Such a term would be most negative near 280 Mev (where $\alpha_{33}\approx 45°$) and zero near 335 Mev (where $\alpha_{33}\approx 90°$). Recent measurements of Corson, Peterson, and McDonald,[20] however, indicate that $B\approx 0$ near 260 Mev and $B\approx 2.7$ μb/sterad at 320 Mev.

This behavior can be explained by the effect of rescattering of charged pions. The "general enhancement model" of Watson *et al.*[19] may be used for illustra-

[49] Explicit formulas for the cross sections will be developed in a paper in preparation by Chew, Low, Goldwasser, and Koester.

[50] M. Ross, Phys. Rev. **103**, 760 (1956). The authors wish to thank Professor Ross for sending a preprint of his work.

tion. Their Eqs. (8–8) include

$$B^0=(4/3)(A_sA_{k0})^{\frac{1}{2}}\{\cos(\alpha_{33}-\alpha_3)-\cos(\alpha_{33}-\alpha_1)+(r+\sqrt{2}r_0)[\cos(\alpha_{33}-\alpha_3)+\tfrac{1}{2}\cos(\alpha_{33}-\alpha_1)-(3/8A_{k0})(A_{k1}+4A_{\Delta 3})]\}. \quad (27)$$

The quantity $(A_{k1}+4A_{\Delta 3})$ is considered negligibly small. Because the magnitudes of the S-phase shifts α_1 and α_3 are small, (27) reduces to

$$B^0\approx-(4/3)(A_sA_{k0})^{\frac{1}{2}}\{(\alpha_3-\alpha_1)\sin\alpha_{33}+(r+\sqrt{2}r_0)[\tfrac{3}{2}\cos\alpha_{33}+(\alpha_3+\tfrac{1}{2}\alpha_1)\sin\alpha_{33}]\}, \quad (28)$$

where $A_s\equiv|E_d^+|^2$ represents the S-wave π^+ photoproduction cross section and A_{k0} the enhanced P-wave contribution interfering with S-waves. The quantity $r=0.113$ is defined by the π^-/π^+ photoproduction ratio, $[\sigma^-(\theta)/\sigma^+(\theta)]_{\text{threshold}}=(1+r)^2$. This r is the part of the nucleon recoil amplitude which changes sign with the meson charge, while r_0 is the part which does not change sign.

The conflict between this recoil term involving $r+\sqrt{2}r_0$ and the charge-exchange scattering term $(\alpha_3-\alpha_1)\sin\alpha_{33}$ results in a slower increase in magnitude with energy, with the rescattering overtaking the recoil in the neighborhood of 260 Mev. The condition $B^0=0$ implies that

$$[(1-\tfrac{1}{2}C)\alpha_1-(1+C)\alpha_3]\tan\alpha_{33}=\tfrac{3}{2}C, \quad (29)$$

where $C=r+\sqrt{2}r_0$. Since $\alpha_1\approx-\alpha_3\approx0.2$ in the energy range 260–280 Mev, and since $\tan\alpha_{33}$ is a rapidly increasing function of energy, the crossing-point energy is relatively insensitive to the value of $r+\sqrt{2}r_0$.

C. Total Cross Sections and the $(\frac{3}{2},\frac{3}{2})$ State

As an illustration of the importance of the $(\frac{3}{2},\frac{3}{2})$ state to the total cross sections, the latter will be used to evaluate the phase shift α_{33}. The Chew-Low cross section (18) can be approximated, within 5%, by the following form:

$$\sigma_T\approx\frac{2\pi}{9}\left(\frac{e^2}{f^2M^2\mu^2}\right)(g_p-g_n)^2\frac{k}{q^3}\sin^2\alpha_{33}, \quad (30)$$

where $\hbar=c=1$, energies are measured in units of μc^2 and momenta in units of μc, μ is the π^0 rest energy, e^2 and f^2 are the electromagnetic and meson-nucleon coupling constants, M is the nucleon rest energy, $g_p=2.78$ and $g_n=-1.91$ are the nucleon magnetic moments in nuclear magnetons, k is the photon momentum, and q is the pion momentum.

Values of α_{33} corresponding to the total cross sections measured in this experiment are plotted in Fig. 12, where they are compared with values measured in scattering experiments.[8] The abscissas are the π^+ bombarding energies, which are related to the incident photon energies by (25). Because α_{33} is strictly defined only for the scattering of π^+ mesons by protons, the values resulting from (30) may differ seriously from the scattering values at pion energies not much greater than the π^+-π^0 mass difference.

ACKNOWLEDGMENTS

The authors wish to thank Professor G. Bernardini and Professor A. O. Hanson for much advice and encouragement, Professor G. F. Chew and Professor F. E. Low for many valuable discussions, and Professor E. L. Goldwasser, Mr. D. Link, and Mr. R. C. Wiquist for assistance in performing the experiment.